Published in final edited form as:
J Control Release. 2012 March 28; 158(3): 487–494. doi:10.1016/j.jconrel.2011.12.011.

Image-guided drug delivery with magnetic resonance guided high intensity focused ultrasound and temperature sensitive liposomes in a rabbit Vx2 tumor model

Ashish Ranjan[1], **Genevieve Jacobs**[1], **David L. Woods**[1], **Ayele H. Negussie**[1], **Ari Partanen**[1,3,4], **Pavel S. Yarmolenko**[1,2], **Carmen E. Gacchina**[1], **Karun V. Sharma**[1], **Victor Frenkel**[5], **Bradford J. Wood**[1], and **Matthew R. Dreher**[1]

[1]Center for Interventional Oncology, Clinical Center and National Cancer Institute, National Institutes of Health, Bethesda, MD [2]Biomedical Engineering, Duke University, Durham, NC [3]Philips Healthcare, Cleveland, OH [4]University of Helsinki, Helsinki, Finland [5]Department of Biomedical Engineering, Catholic University of America, Washington, DC

Abstract

Clinical-grade Doxorubicin encapsulated low temperature sensitive liposomes (LTSLs) were combined with a clinical magnetic resonance-guided high intensity focused ultrasound (MR-HIFU) platform to investigate *in-vivo* image-guided drug delivery. Plasma pharmacokinetics were determined in 3 rabbits. Fifteen rabbits with Vx2 tumors within superficial thigh muscle were randomly assigned into three treatment groups: 1) free doxorubicin, 2) LTSL and 3) LTSL+MR-HIFU. For the LTSL+MR-HIFU group, mild hyperthermia (40–41°C) was applied to the tumors using an MR-HIFU system. Image-guided non-invasive hyperthermia was applied for a total of 30 min, completed within 1 hour after LTSL infusion. High-pressure liquid chromatography (HPLC) analysis of the harvested tumor and organ/tissue homogenates was performed to determine doxorubicin concentration. Fluorescence microscopy was performed to determine doxorubicin spatial distribution in the tumors. Sonication of Vx2 tumors resulted in accurate (mean=40.5±0.1°C) and spatially homogenous (SD=1.0°C) temperature control in the target region. LTSL+MR-HIFU resulted in significantly higher tumor doxorubicin concentrations (7.6- and 3.4-fold greater compared to free doxorubicin and LTSL respectively, $p<0.05$, Newman-Keuls). This improved tumor concentration was achieved despite heating <25% of the tumor volume. Free doxorubicin and LTSL treatments appeared to deliver more drug in the tumor periphery as compared to the tumor core. In contrast, LTSL+MR-HIFU treatment suggested an improved distribution with doxorubicin found in both the tumor periphery and core. Doxorubicin bio-distribution in non-tumor organs/tissues was fairly similar between treatment groups. This technique has potential for clinical translation as an image-guided method to deliver drug to a solid tumor.

Corresponding Author: Dr. Matthew R. Dreher, Staff Scientist, Clinical Center, National Institutes of Health, Radiology and Imaging Sciences, Room 2N212, Building 10, MSC 1182, 9000 Rockville Pike, Bethesda, MD 20892, USA, Phone # (301) 402-8427, Fax # (301) 496-9933, dreherm@cc.nih.gov.

Keywords

Drug Delivery; liposome; MR-HIFU; Vx2 tumor model

1. INTRODUCTION

Current treatment with chemotherapeutic agents in cancer therapy usually relies on systemic delivery with limited tumor specificity, and therefore may result in adverse side effects in normal tissues and insufficient drug delivery to the target tumor [1, 2]. Drug delivery systems (DDS) such as liposomes have been developed to address these challenges, resulting in a number of FDA approved formulations [3]. Encapsulation of a chemotherapeutic agent, such as doxorubicin, into liposomes has the potential to reduce systemic toxicity and enhance drug delivery compared with free drug [4]. In fact, the FDA approval of Doxil (a PEGylated liposomal formulation containing doxorubicin) for the indications of refractory ovarian cancer, AIDS-related Kaposi's Sarcoma, and multiple myeloma was based on equivalent efficacy as standard of care, yet reduced side effects [5].

In contrast to stealth liposomes such as Doxil, which circulate for days and release their drug over weeks, this study focused on temperature sensitive liposomes (TSLs) that release their contents in response to temperature elevations greater than the melting temperature of the lipid formulation [6, 7]. Specifically, we use low temperature sensitive liposomes (LTSLs), which contain a lysolecithin lipid and rapidly release encapsulated doxorubicin upon being heated to mild hyperthermic temperatures (40–42°C) [8]. Previous studies combining LTSLs with local hyperthermia have demonstrated significant reduction in tumor volume in mouse tumor models compared with conventional free drug or non-thermally sensitive liposome therapy [8–11]. Furthermore, mild hyperthermia has been shown to assist drug delivery with liposomes by increasing vascular permeability, resulting in enhanced drug levels in solid tumors [12], and increasing the sensitivity of cancer cells to chemotherapeutics [13]. Therefore, the combination of regionally targeted, image-guided mild hyperthermia (40–42°C) and LTSLs is an attractive and potentially clinically feasible strategy for targeted delivery of doxorubicin to solid tumors.

A variety of methodologies have been developed to achieve local, mild hyperthermia in a solid tumor for combination with TSLs. For example, a warm water bath (~43°C) can achieve mild hyperthermia and drug release in tumor-bearing murine legs [11, 14]. However, in addition to heating a tumor, the water bath approach heats adjoining muscle and skin, as it is not specifically focused on the tumor. Other approaches have been used to circumvent this problem. More tumor specific hyperthermia-mediated drug release has been achieved in canine solid tumors using a clinically relevant scanning annular phased-array microwave applicator [15]. Additionally, LTSLs combined with ultrasound guided, pulsed high intensity focused ultrasound (pulsed-HIFU) resulted in mild hyperthermia and enhanced doxorubicin delivery and antitumor effects in a murine solid tumor model [16]. The complex bio-effects of ultrasound include heat generation, acoustic cavitation, and radiation forces [17], all of which may theoretically be employed to improve drug delivery [18–20].

Despite many technological advances, current hyperthermia applicators are often limited in their ability to provide a spatially accurate or deep thermal therapy to a solid tumor. To address these challenges, HIFU has been combined with magnetic resonance imaging (MRI) in an integrated MR-guided high intensity focused ultrasound (MR-HIFU) system [21, 22]. This approach uses MRI to acquire images of anatomy and targets for treatment planning, and to perform temperature imaging for treatment monitoring and control. This control may

provide a more consistent HIFU treatment whose bio-effects are intimately related to time and temperature exposures. MR-HIFU has more commonly been used as an ablative therapy (>60 °C), but more recently, the MR-HIFU systems have been developed or modified to target mild hyperthermia to deep tissue, for potential combination with TSLs [23–25].

The *objective* of this study was to investigate the combination of a clinical MR-HIFU system with an LTSL that is currently in phase III clinical trials [26] in a Vx2 rabbit tumor model. This is an important step to translate this image-guided drug delivery approach to the clinic. Image-guided drug delivery is an exciting and emerging field [19, 27] that may provide the advantage of better tumor specificity or spatial targeting, when compared with more traditional drug delivery strategies.

2. MATERIALS AND METHODS

2.1. Chemicals

A lyso-lecithin containing LTSL formulation (ThermoDox®, Celsion Corp., USA) was provided through a Collaborative Research and Development Agreement at a concentration of 1.8 mg doxorubicin/mL. Doxorubicin hydrochloride (Doxorubicin), zinc sulfate monohydrate ($ZnSO_4$), phosphate buffer saline (PBS), potassium phosphate monobasic (KH_2PO_4), nitroblue tetrazolium (NBT), magnesium chloride ($MgCl_2$), nicotinamide adenine dinucleotide phosphate (NADPH), and Trifluoroacetic acid were obtained from Sigma-Aldrich (Saint Louis, MO, USA). Similarly, HPLC-grade acetonitrile and daunurobicin hydrochloride (DNR) for internal standard (IS) were obtained from VWR international (Swedesboro, NJ, USA). For Vx2 (kind gift from Dr. Jeff Geschwind, Johns Hopkins University) cell preparation, PEB buffer was obtained from Miltenyl Biotech (Auburn, CA, USA). For histopathology, prolong Gold with DAPI mounting medium was obtained from Invitrogen (Carlsbad, CA, USA).

2.2. Animal and Tumor Model

All animal-related procedures were approved and carried out under the guidelines of the National Institutes of Health (NIH) Animal Care and Use Committee. All image guided drug delivery studies were performed in New Zealand White Rabbit with Vx2 tumor in hind limb.

2.2.1. Preparation of Vx2 Single Cell Suspension—The Vx2 tumor cell solution was prepared with the following technique. The donor animal bearing a tumor > 1cm in size was anesthetized with a mixture of pre-anesthetics (28.6 mg/kg ketamin.e HCl [Bioniche Teoranta, Inverin, Co. Galway, Ireland], 4.8 mg/kg xylazine [Lloyd laboratory, Shenandoah, Iowa, USA], intramuscular [I.M.]). Following onset of anesthesia, both hind limbs were shaved and underwent aseptic preparation in a BSL-2 hood. Midline and horizontal incisions were made through the skin where the tumor was implanted, and the skin flap was pulled back exposing the tumor mass. The tumor was freed from surrounding muscle by careful dissection and transferred to a sterile petri dish containing 10–15 mL of PEB buffer. Once both tumors were excised, the animal was immediately euthanized by intravenous injection of Euthanasia III (dose = 0.2 mL/kg, Pentobarbital Sodium 390 mg/ml and Phenytoin Sodium 50 mg/ml, Med-Pharmax, inc., Pomona, CA, USA). Later, the harvested Vx2 tumor fragment was cut free of normal fascia and any necrotic material, minced into approximately 2 × 2 × 2 mm cubes, immediately transferred into a gentleMACS C Tube and dissociated according to the mouse tumor protocol (m_impTumor_01 protocol, Miltenyi Biotec, CA, USA). The resulting cell suspension was counted and evaluated using Trypan blue exclusion test before being separated into 1.5-mL vials in 150-μL aliquots of cells in PBS or PEB. The vials were immediately placed on ice and transported to the animal facility for inoculation.

2.2.2. Inoculation and Monitoring—For inoculations, the hind limb was shaved and cleaned with 70% isopropyl alcohol. For donor rabbit, Vx2 tumor cells (150–200 μL, ~2–3 million cells) were propagated and maintained by bilateral hind limb inoculation. For the drug delivery experiments, ~ 2–3 million Vx2 cells were injected into the superficial thigh muscle of right hind limb under ultrasound guidance (Sonosite M Turbo, Bothell, WA, USA). Tumor growth was monitored with ultrasound for 2–3 weeks and experiments were performed when the tumor was greater than 1 cm in any dimension.

2.3. Tumor Drug Delivery Study design

15 New Zealand White Rabbits, with Vx2 tumors, were randomly assigned into three treatment groups (5 rabbits/group): 1) free doxorubicin, 2) LTSL and 3) LTSL+ MR-HIFU hyperthermia. In all groups, 5 mg doxorubicin/kg body weight was administered intravenously.

2.4. Image Guided Hyperthermia

2.4.1. *In-vivo* Experiment Setup—For image-guided MR-HIFU hyperthermia, the rabbit was anesthetized with a mixture of ketamine and xylazine (28.6 mg/kg ketamine, 4.8 mg/kg xylazine, I.M.). Marginal ear vein was catheterized, and the tumor bearing leg was shaved and treated with Nair™ (Church & Dwight Co., NJ, USA). Once positioned in the MR scanner (Achieva 1.5 T, Philips Healthcare, Best, the Netherlands), anesthesia was maintained with 1–3% isoflurane using a mask. Body (rectal) and water bath temperatures were monitored using fiber optic probes (T1 Fiber Optic Temperature Sensor and Reflex™ Signal Conditioner, Neoptix, Québec City, Québec, Canada). A third optical temperature probe (diameter = 0.56 mm, Luxtron 3100, LumaSense Technologies, Santa Clara, CA, USA) was placed in the thigh muscle near the tumor and used as a baseline temperature for MR thermometry, prior to each sonication. Vital signs were monitored with an MR-compatible patient monitoring system (Precess, In-vivo, Orlando, FL, USA) using a fiber optic cuff placed around the shaved area of the animal's front paw.

2.4.2. Treatment Planning and Schedule—An integrated MR-HIFU clinical platform (Sonalleve 1.5T, Philips Medical Systems, Vantaa, Finland) was used for tumor identification, sonications with MR guidance, and treatment characterization. The tumor-bearing limb was partly submerged in a bath of degassed water to provide acoustic coupling, and sonications were targeted to the center of tumor using custom modified commercial treatment planning software (Fig. 1).

A high resolution 3D turbo spin echo pulse sequence was used for treatment planning (TR=1600ms, TE=30ms, slice thickness = 2mm, 120 slices, FOV = 20×20cm, matrix = 640×640, NEX=1). LTSL solution (5 mg doxorubicin/kg) was slowly administered over a span of 3 min, followed by a 1 mL saline flush. Subsequently, 10 min MR-HIFU hyperthermia treatment blocks were performed, each followed by a 5 min cooling period, allowing temperature in the heated region to return to baseline, as verified with MR thermometry. A total of 30 min of heating was completed within 1 hour of drug infusion (Fig. 2). Some of the heating sessions were prematurely aborted due to animal movement (MR thermometry's accuracy is very sensitive to movement). In such cases, the aborted 10 min treatment was completed following a 5 min cooling period, always within 60 min of drug infusion. Three separate 10 min. hyperthermia treatments were used to obtain a new baseline image for temperature imaging, limiting the potential influence of magnetic drift or motion.

2.4.3. Control of Mild Hyperthermia with MR-HIFU—HIFU beam was electronically steered in a circular trajectory to heat a 4 mm region in the tumor (Fig. 3) of each rabbit for up to 10 minute blocks [22].

Temperature maps were obtained in coronal and sagittal planes using the proton resonance frequency shift (PRFS) method [28] and a 2D echo planar fast field echo (FFE-EPI) pulse sequence (TR=54 ms, TE=30 ms, flip angle=19°, slice thickness=7 mm, in-plane resolution=1.39×1.39 mm, temporal resolution=2.5 s, EPI factor =7, number of slices =2). An unheated region in the flank muscle was monitored to correct for magnetic drift. Core body temperature was maintained between 34 and 37°C (described below in section 2.5). Mean temperature in the target region within the coronal slice was maintained using a binary feedback algorithm. This algorithm triggered heating when the mean temperature was ≤40°C, and did not heat when mean temperature was ≥41°C in the prescribed region. Temperature maps were analyzed for spatial targeting accuracy (offset), temperature accuracy (mean) and homogeneity of heating (standard deviation (SD), 10^{th} percentile (T10) and 90^{th} percentile (T90)) from the point when the mean temperature reached 39°C to the end of sonication.

2.4.4. Post-Treatment Procedures—Following treatment, the rabbit was removed from the bore of the magnet and transferred to an animal procedure room. An additional dose of ketamine and xylazine (28.6 mg/kg ketamine, 4.8 mg/kg xylazine, I.M.) was administered to keep the animal anesthetized during transfer. The animal was then maintained on 1–2 % isofluorane anesthesia and monitored until 4 hours post LTSL infusion. The animal was then euthanized using Euthanasia III (dose = 0.2 ml/kg, Pentobarbital Sodium 390 mg/ml and Phenytoin Sodium 50 mg/ml). The tumor and tissues samples from liver, spleen, lung, heart, kidney, skin and muscle both adjacent and contra-lateral to the heated tumor were excised, weighed, snap frozen over liquid nitrogen, and then stored at −80°C until histopathology and HPLC analysis.

2.5. Non-Hyperthermia Drug Delivery Procedures

Animal experiments with free doxorubicin and LTSL without hyperthermia were performed outside of the MRI magnet. Following onset of anesthesia, the core-body temperature was maintained between 34 and 37°C through the use of a heating blanket (on the side of non-tumor-bearing leg) or ice for cooling. Doxorubicin (5 mg doxorubicin/kg) was infused via the marginal ear vein over the course of 3 min followed by a 1 mL saline flush. Body temperature, breathing and heart rates were monitored.

2.6. Plasma Pharmacokinetics of LTSL

For pharmacokinetic evaluations, 3 healthy rabbits under experimental conditions similar to non-hyperthermia procedure were infused with LTSLs at a Doxorubicin dosage of 5 mg/kg body weight. One mL of blood from the central ear artery was withdrawn into an EDTA-containing vacutainer tube (Becton Dickinson Vacutainer Systems, Franklin Lakes, NJ, USA) at time 0 (before infusion), immediately after completion of the infusion, and at 15, 30, 60, 90, 120, 180 and 240 min after LTSL infusion. Immediately after blood collection, the tube was placed on ice, blood was centrifuged at 2000 × g for 10 min at 4°C, plasma was then removed and stored at −80°C until further analysis. Doxorubicin concentration in plasma versus time was fit to a one-compartment model with first-order elimination using least-squares non-linear regression analysis with GraphPad Prism 5.0 (GraphPad Software Inc., San Diego, CA, USA). The area under the curve (AUC) between 0 to 240 min was calculated using the trapezoidal rule in GraphPad. Total systemic clearance was calculated as dose/AUC.

2.7. Quantification of Doxorubicin by HPLC

Tissue homogenization and sample preparation for HPLC was carried out as previously reported [29] with slight modifications. Briefly, samples were homogenized, doxorubicin extracted and quantified with HPLC using an internal standard DNR. Additional information may be found in supplemental information.

2.8. Histological and Fluorescent Microscopy Analysis

Vx2 tumors from rabbits treated either with free doxorubicin, LTSL alone, or LTSL+MR-HIFU were harvested within 15 min of euthanasia (4 hours after administration), flash frozen in liquid nitrogen, and stored at −80°C until further processing. Serial sections of 8 μm thickness were obtained. Hematoxylin and eosin staining (H & E) was completed using a standard protocol for gross histological assessment of cellular density, necrosis, and fibrosis. Regions of necrosis were also identified using NBT-based viability staining as described previously [30]. Whole section digital histological scans were acquired with a 20X objective on a ScanScope CS (Aperio, Vista, CA) equipped with a color CCD camera and image processing software (ImageScope, Aperio). Additionally, epi-fluorescence imaging of cell nuclei (Prolong Gold Mounting Medium with DAPI) and doxorubicin distribution (excitation 480/40nm, emission 600/60nm, and dichroic 505lp) was conducted. Image acquisition and display parameters were constant for doxorubicin imaging to allow for qualitative comparison (n=1). All imaging was performed with 5X and 10X objectives on a upright microscope (Zeiss, Axio Imager.M1, Thornwood, NY) equipped with a color CCD camera, cooled monochrome CCD camera, motorized scanning stage, and mosaic stitching software (Axiovision, Zeiss).

3.0 STATISTICAL ANALYSIS

Treatment groups were compared for differences in mean tumor doxorubicin concentration using analysis of variance (ANOVA) followed by Newman-Keuls multiple comparison post-hoc test. All analyses were performed using GraphPad Prism 5.0 (GraphPad Software Inc.). All *p*-values were two-sided, and a *p*-value less than 0.05 indicated statistical significance. Values are reported as mean ± SEM unless otherwise indicated.

4. RESULTS

4.1 Image-Guided Hyperthermia

The mild hyperthermia heating algorithm resulted in an accurate (40.5 ± 0.1 °C, target = 40 – 41 °C) and homogeneous (SD = 1.0 °C) temperature within the targeted region of interest (ROI), with a mean 3D spatial offset of 1.1 ± 0.1 mm (n=5). The T10 and T90 within the ROI were 41.8 ± 0.1 °C and 39.2 ± 0.2 °C, respectively, demonstrating tight temperature control. Fig. 4 shows a representative example of mean temperature elevation during a sonication together with T10 and T90, and mean spatial temperature distribution. It took approximately 15–20 seconds to achieve the target temperature range of 40–41 °C, after which the temperature was maintained consistently by the binary feedback controller (Fig 4A). Also, the mean spatial temperature distribution was very uniform and corresponded with the desired treatment region, as indicated by the dotted circle (Fig. 4B).

4.2 Pharmacokinetics and Biodistribution of Doxorubicin

Plasma pharmacokinetics of doxorubicin in an LTSL formulation was evaluated with reverse phase HPLC from plasma after intravenous administration. Plasma doxorubicin concentration was highest (C_{max}) at the completion of infusion and slowly decreased thereafter (Fig. 5). In contrast to doxorubicin which demonstrates a rapid initial clearance of >95% in ~5min [31], an LTSL formulation decreased 88% over a 4 hour time period. Most

importantly, the plasma concentration was >75% of C_{max} over the first hour, corresponding to the prescribed MR-HIFU treatment duration. The initial volume of distribution 58 ± 12 mL/kg was nearly similar to the predicted plasma volume of a rabbit of this body weight 37.3 ± 4.4 mL/kg [32]. Such findings are consistent with the apparent volume of distribution reported previously for non-thermosensitive liposomes (Doxil) [33].

Doxorubicin biodistribution was determined in liver, kidney, spleen, heart, tissues (muscle and skin) adjoining and contra-lateral to tumor in all treatment groups (n=5). Doxorubicin levels were similar in the kidney, heart, spleen, muscle and skin adjoining and contra-lateral to the tumor for various treatment groups ($p>0.05$, Newman-Keuls) (Fig.6).

Treatment with LTSL alone resulted in significantly higher accumulation (1.8-fold) ($p<0.05$, Newman-Keuls) in liver compared to free doxorubicin. LTSL+MR-HIFU treatment resulted in significantly greater doxorubicin delivery to lung compared to free doxorubicin (1.4-fold) or LTSL alone (1.5-fold) treatments ($p<0.05$, Newman-Keuls). All other pair-wise comparisons in liver and lung were not significant ($p>0.05$, Newman-Keuls). For exact doxorubicin concentration values and %ID/g, please see supplemental table 1.

4.3 Tumor Drug Delivery

Tumor doxorubicin concentrations were 4.0 ± 1.0, 8.8 ± 1.4, 30 ± 9 μg doxorubicin/g tissue for free doxorubicin, LTSL and LTSL+MR-HIFU, respectively (Fig 7). LTSL+MR-HIFU resulted in a 7.6-fold greater tumor drug delivery compared to free doxorubicin ($p<0.05$, Newman-Keuls) and 3.4-fold greater delivery compared to LTSL alone ($p<0.05$, Newman-Keuls) (Fig. 7). In terms of specificity of drug delivery to a tumor compared to muscle (tumor: adjoining muscle), the relative doxorubicin concentrations were 4.3-, 12.5-, and 43.5-fold greater for free doxorubicin, LTSL, and LTSL+MR-HIFU groups, respectively (Fig. 8). The specificity of LTSL+MR-HIFU was significantly greater than the other treatments ($p<0.05$, Newman-Keuls).

4.4 Histopathology Analysis

H&E staining demonstrated tumor encased in hind limb muscle mass (Fig. 9a–c) consisting of both viable and necrotic tumor tissue and a well-defined tumor border adjacent to normal muscle tissue (n=1). To better identify viable tumor tissue, NADH viability staining was used to differentiate the viable (blue regions) and nonviable (white/clear regions) tumor tissue (Fig. 9d–f). Viability staining indicated that the extent of tumor necrosis was similar in the various treatment groups (n=1). The fluorescence images of doxorubicin illustrated heterogeneous drug distribution (n=1; Fig 9i & l). The intensity of doxorubicin in tumor (red), appeared to be greatest in the LTSL+MR-HIFU group. Doxorubicin appeared to preferentially accumulate in tumor periphery following free doxorubicin and LTSL treatments. In contrast, an LTSL+MR-HIFU treatment appeared to increase doxorubicin fluorescence intensity in the periphery as well as tumor core, suggesting improved intra-tumoral distribution. A comparison of the viability stain (Fig. 9a–f) to the fluorescence microscopy images on serial sections suggests greatest doxorubicin fluorescence intensity in viable areas. Drug distribution in tumors appeared spatially inhomogeneous in all groups (Fig. 9g–l).

5. DISCUSSION

The *objective* of this study was to investigate the feasibility of combining a clinical MR-HIFU system with a clinical-grade LTSL formulation in a relevant tumor model that reproduces the geometries and scales of typical cancer patients (e.g., tumor encased in normal tissue). This study could potentially aid in translation of this image-guided focal

drug delivery paradigm to the clinic. These findings provide background and preliminary foundation for future clinical trial design.

5.1 Choice of Tumor Models, Liposomes and MR-HIFU System

Clinical translation of MR-HIFU-mediated drug delivery requires a series of pre-clinical studies with an appropriate animal model to rigorously evaluate the shortcomings, pitfalls, and hurdles, as well as potential advantages. Notable contributions to date include the use of clinical-grade LTSLs and a modified pre-clinical MR-HIFU system in a normal rabbit thigh muscle [23] as well as TSLs and a clinical MR-HIFU system in a rat tumor model [24]. Results from these studies [23, 24] and those presented herein are consistent and demonstrate the ability to use MR-HIFU to enhance drug delivery. The rabbit Vx2 tumor model has the added value of evaluating spatio-temporal control of heating and subsequent drug delivery to a large tumor encased in skeletal muscle (unlike most rodent models). In fact high concentrations of doxorubicin were achieved in the tumor while sparing intervening skin and adjacent muscle, demonstrating the ability to selectively deliver and "paint" drug to the desired region with advanced image guidance using clinical MR imaging.

Spatial and thermal accuracy of the MR-HIFU system is a prerequisite for fully leveraging the advantages of image-guided drug delivery. The clinical MR-HIFU system was capable of accurate spatial targeting the desired tissue (spatial offset = 1.1 ± 0.1 mm) and delivering the desired temperature elevations (40.5 ± 0.1°C) and homogeneity of heating (SD = 1.0 °C). As shown in Fig 3, the desired region was heated, yet this did not correspond to the entire tumor volume. Drug delivery could be further improved if the entire tumor volume was heated. Therefore, the ability to deliver large volume conformal mild hyperthermia treatments may be necessary to fully realize the potential of this strategy for addressing unmet clinical needs in the local and regional treatment of cancer.

A clinical-grade LTSL formulation, which contains a lysolecithin lipid, was used herein [8, 10], yet there are numerous TSL formulations being investigated. More recently, TSL formulations have been reported that may provide for longer circulation, albeit with possibly slower release rates [34, 35]. Additionally, image-able TSL formulations are being developed for image-guided drug delivery with potential for real-time monitoring. Dewhirst and colleagues have demonstrated the ability to image drug delivery with MRI using manganese-loaded LTSLs [36, 37]. More recently, LTSLs loaded with gadolinium-based MR contrast agents and Doxorubicin have been demonstrated in-vivo in combination with MR-HIFU [24, 25]. These gadolinium-based formulations have a better chance of clinical translation than manganese, due to toxicity concerns, and therefore should be explored further. Further optimization of image-guided hyperthermia and long circulating liposomes could potentially improve local drug delivery and limit systemic side effects.

5.2 Drug Transport

Drug delivery to tumor using liposomes largely depends on the liposome plasma circulation half-life and the rate of release of the encapsulated drug, among other factors [38]. The combination of rapid release LTSLs and hyperthermia results in intravascular release of doxorubicin followed by transport of doxorubicin across the endothelial barrier and through the extravascular extracellular space followed by cellular uptake [13, 39, 40]. Therefore, the penetration and coverage of cytotoxic concentrations of doxorubicin into the tumor would be optimized if the drug was released at peak plasma LTSL concentration. Furthermore, complete release from an LTSL occured on the timescale comparable to the mean tumor transit time, highlighting the importance (if not requirement) of fast release in order for an intravascular mechanism to function effectively [13]. A comparison of the pharmacokinetic

profile (Fig. 5) and the treatment scheme (Fig. 2) suggests that delivery occurred while the plasma concentration was near its C_{max}. Liposomes that exhibit slower release and longer plasma half-life may first accumulate in a tumor through the EPR effect, followed by extravascular release upon heating [35]. Both strategies have merits, but further investigation may be required to determine the benefits or the optimal balance of each strategy.

Fluorescence microscopy demonstrated that doxorubicin was heterogeneously distributed within the tumor for all treatment groups. Much greater doxorubicin signal was observed in the LTSL+MR-HIFU group, consistent with the quantitative and statistically significant HPLC analysis ($P<0.05$). Enhanced localization to the tumor periphery was seen, possibly related to the fact that tumor periphery is often locally well perfused. This preference for tumor periphery was particularly evident in the tumors treated with free doxorubicin and LTSL alone. Interestingly, tumors heated with LTSL+MR-HIFU showed greater doxorubicin fluorescence in the tumor core (Fig. 9i&l), which is often a difficult location to deliver drugs, given its tendency to be less perfused and exhibit high interstitial pressures (IFP). Although the fluorescence in general corresponded to the heated location, a precise spatial correlation was not performed. Since the evaluation of doxorubicin distribution was done in a single tumor treated in each group, these observations are thus inconclusive. One possible explanation is that hyperthermia reduced IFP [41] and improved tumor perfusion [42]. The combination therapy of LTSL+MR-HIFU may have increased perfusion to the tumor core and established a high intravascular drug concentration leading to the improved drug coverage observed in the tumor core.

5.3 Specificity of Drug Delivery

The underlying motivation for conducting a doxorubicin biodistribution in the present study was to evaluate both potential tumor therapy and normal tissue side effects. LTSL+MR-HIFU resulted in 3.5- to 7.6-fold more tumor doxorubicin delivery than LTSL and doxorubicin groups, respectively. In addition, following LTSL+ MR-HIFU we observed ~43-fold higher doxorubicin concentration in tumor, compared to adjoining muscle (Fig. 8). This suggests that the drug delivery was highly target-specific, which could have important implications and advantages for this treatment paradigm. Also, doxorubicin concentration in normal tissues was largely similar between the treatment groups (within 20–80%). Presumably, the safety profile of LTSL+MR-HIFU may be similar to free doxorubicin therapy but with an added benefit of more drug exposure in the tumor. Stealth, long-circulating liposomes are often thought to improve the safety profile [5]. Additional studies are warranted to characterize and evaluate strategies for both decreasing systemic exposure and maintaining a high level of tumor drug delivery. Long circulating TSLs formulations may limit systemic toxicity, similar to Doxil [5], while improving tumor drug delivery.

This LTSL + MR-HIFU drug delivery strategy has ample room for improvement. Importantly, only a fractional portion of the entire tumor volume (<25%) was heated due to limitations of the current MR-HIFU system. Despite this shortcoming, significantly greater drug delivery to tumor was achieved with MR-HIFU (7.6-fold greater compared to free doxorubicin). Segmental analysis of one tumor demonstrated quite variable drug concentrations (mean = 26 μg/g, range =11.9 – 63.2 μg/g) suggesting that large volume conformal heating of the entire tumor may further improve drug delivery but this approach would require further hardware and software development that is currently in progress.

The potential of image-guided focally selective drug delivery has yet to be realized. This drug and device combination allows for precise spatial targeting of tumor regions while sparing adjacent normal tissue. Pre-procedural imaging, including DCE-MRI, hypoxia, metabolism and ADC maps [43] may be used to quantify tumor biological, physiologic, and

mass transport properties to be used in a treatment plan to customize the therapy to an individual patient. For example, ADC maps could help define less well-vascularized tissue that may be better treated with ablation techniques whereas DCE-MRI might reveal highly enhancing tumor tissue that may be better treated through vascular delivery of heat-deployed drug. Image-able TSL formulations [24, 25] may report on drug delivery in real-time to refine the treatment during the procedure or to guide future interventions. The use of image-guidance in focal drug delivery is in its infancy, yet has the potential to improve personalized cancer therapies [19, 27, 44, 45].

6. CONCLUSION

This work demonstrated the feasibility of combining a clinical MR-HIFU and a clinical-grade LTSL in a relevant Vx2 rabbit tumor model. Stable and spatially accurate mild hyperthermia with MR-HIFU significantly improved delivery of doxorubicin to tumor tissue while sparing adjacent normal tissue. This image-guided drug delivery technique combines drug and device in a rational approach that has potential for clinical translation.

Supplementary Material

Refer to Web version on PubMed Central for supplementary material.

Acknowledgments

This research was supported by the Center for Interventional Oncology in the Intramural Research Program of the National Institutes of Health (NIH). NIH and Celsion Corp. have a Cooperative Research and Development Agreement. NIH and Philips Healthcare have a Cooperative Research and Development Agreement. We thank Dr. Mark Dewhirst, Dr. Ivan Spasojevic and Dr. Sham Sokka for their advice and useful discussions. We also thank Dr. Max Köhler, Julia Enholm, and Jaakko Tölö of Philips Healthcare for their support and technical expertise. We would also like to thank Dr. James Coad for providing us with a viability staining protocol.

References

1. Bae YH, Park K. Targeted drug delivery to tumors: myths, reality and possibility. Journal of Controlled Release. 2011; 153:198–205. [PubMed: 21663778]
2. Allen TM, Cullis PR. Drug delivery systems: Entering the mainstream. Science. 2004; 303(5665): 1818–1822. [PubMed: 15031496]
3. Drummond DC, Meyer O, Hong K, Kirpotin DB, Papahadjopoulos D. Optimizing liposomes for delivery of chemotherapeutic agents to solid tumors. Pharmacol Rev. 1999; 51(4):691–743. [PubMed: 10581328]
4. Jain RK, Stylianopoulos T. Delivering nanomedicine to solid tumors. Nat Rev Clin Oncol. 2010; 7(11):653–664. [PubMed: 20838415]
5. O'Brien ME, Wigler N, Inbar M, Rosso R, Grischke E, Santoro A, Catane R, Kieback DG, Tomczak P, Ackland SP, Orlandi F, Mellars L, Alland L, Tendler C. Reduced cardiotoxicity and comparable efficacy in a phase III trial of pegylated liposomal doxorubicin HCl (CAELYX/Doxil) versus conventional doxorubicin for first-line treatment of metastatic breast cancer. Ann Oncol. 2004; 15(3):440–449. [PubMed: 14998846]
6. Yatvin MB, Weinstein JN, Dennis WH, Blumenthal R. Design of liposomes for enhanced local release of drugs by hyperthermia. Science. 1978; 202(4374):1290–1293. [PubMed: 364652]
7. Weinstein JN, Magin RL, Yatvin MB, Zaharko DS. Liposomes and local hyperthermia: selective delivery of methotrexate to heated tumors. Science. 1979; 204(4389):188–191. [PubMed: 432641]
8. Kong G, Anyarambhatla G, Petros WP, Braun RD, Colvin OM, Needham D, Dewhirst MW. Efficacy of liposomes and hyperthermia in a human tumor xenograft model: importance of triggered drug release. Cancer Res. 2000; 60(24):6950–6957. [PubMed: 11156395]

9. Chelvi TP, Jain SK, Ralhan R. Hyperthermia-mediated targeted delivery of thermosensitive liposome-encapsulated melphalan in murine tumors. Oncol Res. 1995; 7(7–8):393–398. [PubMed: 8747602]
10. Needham D, Anyarambhatla G, Kong G, Dewhirst MW. A new temperature-sensitive liposome for use with mild hyperthermia: characterization and testing in a human tumor xenograft model. Cancer Res. 2000; 60(5):1197–1201. [PubMed: 10728674]
11. Yarmolenko PS, Zhao Y, Landon C, Spasojevic I, Yuan F, Needham D, Viglianti BL, Dewhirst MW. Comparative effects of thermosensitive doxorubicin-containing liposomes and hyperthermia in human and murine tumours. Int J Hyperthermia. 2010; 26(5):485–498. [PubMed: 20597627]
12. Kong G, Braun RD, Dewhirst MW. Characterization of the effect of hyperthermia on nanoparticle extravasation from tumor vasculature. Cancer Res. 2001; 61(7):3027–3032. [PubMed: 11306483]
13. Landon CD, Park JY, Needham D, Dewhirst MW. Drug Delivery and Hyperthermia: The Materials Design and Preclinical and Clinical Testing of Low Temperature-Sensitive Liposomes Used in Combination with Mild Hyperthermia in the treatment of Local. The open Nanomedicine Journal. 2011; 3:38–64.
14. Horsman MR, Murata R, Overgaard J. Improving local tumor control by combining vascular targeting drugs, mild hyperthermia and radiation. Acta Oncol. 2001; 40(4):497–503. [PubMed: 11504310]
15. Hauck ML, LaRue SM, Petros WP, Poulson JM, Yu D, Spasojevic I, Pruitt AF, Klein A, Case B, Thrall DE, Needham D, Dewhirst MW. Phase I trial of doxorubicin-containing low temperature sensitive liposomes in spontaneous canine tumors. Clin Cancer Res. 2006; 12(13):4004–4010. [PubMed: 16818699]
16. Dromi S, Frenkel V, Luk A, Traughber B, Angstadt M, Bur M, Poff J, Xie J, Libutti SK, Li KC, Wood BJ. Pulsed-high intensity focused ultrasound and low temperature-sensitive liposomes for enhanced targeted drug delivery and antitumor effect. Clin Cancer Res. 2007; 13(9):2722–2727. [PubMed: 17473205]
17. O'Brien WD Jr. Ultrasound-biophysics mechanisms. Prog Biophys Mol Biol. 2007; 93(1–3):212–255. [PubMed: 16934858]
18. Frenkel V. Ultrasound mediated delivery of drugs and genes to solid tumors. Adv Drug Deliv Rev. 2008; 60(10):1193–1208. [PubMed: 18474406]
19. Deckers R, Moonen CT. Ultrasound triggered, image guided, local drug delivery. J Control Release. 2003; 148(1):25–33. [PubMed: 20709123]
20. Ferrara KW. Driving delivery vehicles with ultrasound. Adv Drug Deliv Rev. 2008; 60(10):1097–1102. [PubMed: 18479775]
21. Quesson B, Laurent C, Maclair G, de Senneville BD, Mougenot C, Ries M, Carteret T, Rullier A, Moonen CTW. Real-time volumetric MRI thermometry of focused ultrasound ablation in vivo: a feasibility study in pig liver and kidney. Nmr in Biomedicine. 2011; 24(2):145–153. [PubMed: 21344531]
22. Kohler MO, Mougenot C, Quesson B, Enholm J, Le Bail B, Laurent C, Moonen CT, Ehnholm GJ. Volumetric HIFU ablation under 3D guidance of rapid MRI thermometry. Med Phys. 2009; 36(8):3521–3535. [PubMed: 19746786]
23. Staruch R, Chopra R, Hynynen K. Localised drug release using MRI-controlled focused ultrasound hyperthermia. Int J Hyperthermia. 2011; 27(2):156–171. [PubMed: 21158487]
24. de Smet M, Heijman E, Langereis S, Hijnen NM, Grull H. Magnetic resonance imaging of high intensity focused ultrasound mediated drug delivery from temperature-sensitive liposomes: an in vivo proof-of-concept study. J Control Release. 2011; 150(1):102–110. [PubMed: 21059375]
25. Negussie AH, Yarmolenko PS, Partanen A, Ranjan A, Jacobs G, Woods D, Bryant H, Thomasson D, Dewhirst MW, Wood BJ, Dreher MR. Formulation and characterisation of magnetic resonance imageable thermally sensitive liposomes for use with magnetic resonance-guided high intensity focused ultrasound. Int J Hyperthermia. 2011; 27(2):140–155. [PubMed: 21314334]
26. Celsion. A Phase III, Randomized, Double-Blinded, Dummy-Controlled Study of the Efficacy and Safety of ThermoDox® (Thermally Sensitive Liposomal Doxorubicin) in Combination With Radiofrequency Ablation (RFA) Compared to RFA-Alone in the Treatment of Non-Resectable Hepatocellular Carcinoma. 2011. http://clinicaltrials.gov/ct2/show/NCT00617981>

27. Tandon P, Farahani K. NCI Image-Guided Drug Delivery Summit. Cancer Res. 2011; 71(2):314–317. [PubMed: 21224356]
28. Ishihara Y, Calderon A, Watanabe H, Okamoto K, Suzuki Y, Kuroda K. Precise and Fast Temperature Mapping Using Water Proton Chemical-Shift. Magnetic Resonance in Medicine. 1995; 34(6):814–823. [PubMed: 8598808]
29. Kuh HJ, Al-Abd AM, Kim NH, Song SC, Lee SJ. A simple HPLC method for doxorubicin in plasma and tissues of nude mice. Archives of Pharmacal Research. 2009; 32(4):605–611. [PubMed: 19407979]
30. Coad JE, Garza-Leal J, Hernandez I, Castillo L, Jessop ML, Chill N. Successful Vapor-Based Endometrial Ablation: In Vivo Peri-Hysterectomy Study. Journal of Minimally Invasive Gynecology. 2011; 18(4):445–448. [PubMed: 21777834]
31. Speth PA, van Hoesel QG, Haanen C. Clinical pharmacokinetics of doxorubicin. Clin Pharmacokinet. 1988; 15(1):15–31. [PubMed: 3042244]
32. Prince H. Blood volume in the pregnant rabbit. Q J Exp Physiol. 1982; 67(1):87–95. [PubMed: 7079452]
33. Gabizon A, Shmeeda H, Barenholz Y. Pharmacokinetics of pegylated liposomal Doxorubicin: review of animal and human studies. Clin Pharmacokinet. 2003; 42(5):419–436. [PubMed: 12739982]
34. Lindner LH, Eichhorn ME, Eibl H, Teichert N, Schmitt-Sody M, Issels RD, Dellian M. Novel temperature-sensitive liposomes with prolonged circulation time. Clin Cancer Res. 2004; 10(6): 2168–2178. [PubMed: 15041738]
35. Koning GA, Eggermont AM, Lindner LH, ten Hagen TL. Hyperthermia and thermosensitive liposomes for improved delivery of chemotherapeutic drugs to solid tumors. Pharm Res. 2010; 27(8):1750–1754. [PubMed: 20424894]
36. Viglianti BL, Abraham SA, Michelich CR, Yarmolenko PS, MacFall JR, Bally MB, Dewhirst MW. In vivo monitoring of tissue pharmacokinetics of liposome/drug using MRI: illustration of targeted delivery. Magn Reson Med. 2004; 51(6):1153–1162. [PubMed: 15170835]
37. Ponce AM, Viglianti BL, Yu D, Yarmolenko PS, Michelich CR, Woo J, Bally MB, Dewhirst MW. Magnetic resonance imaging of temperature-sensitive liposome release: drug dose painting and antitumor effects. J Natl Cancer Inst. 2007; 99(1):53–63. [PubMed: 17202113]
38. Charrois GJ, Allen TM. Drug release rate influences the pharmacokinetics, biodistribution, therapeutic activity, and toxicity of pegylated liposomal doxorubicin formulations in murine breast cancer. Biochim Biophys Acta. 2004; 1663(1–2):167–177. [PubMed: 15157619]
39. Chen Q, Tong S, Dewhirst MW, Yuan F. Targeting tumor microvessels using doxorubicin encapsulated in a novel thermosensitive liposome. Mol Cancer Ther. 2004; 3(10):1311–1317. [PubMed: 15486198]
40. Gasselhuber A, Dreher MR, Negussie A, Wood BJ, Rattay F, Haemmerich D. Mathematical spatio-temporal model of drug delivery from low temperature sensitive liposomes during radiofrequency tumour ablation. Int J Hyperthermia. 2010; 26(5):499–513. [PubMed: 20377363]
41. Sen A, Capitano ML, Spernyak JA, Schueckler JT, Thomas S, Singh AK, Evans SS, Hylander BL, Repasky EA. Mild elevation of body temperature reduces tumor interstitial fluid pressure and hypoxia and enhances efficacy of radiotherapy in murine tumor models. Cancer Res. 2011; 71(11): 3872–3880. [PubMed: 21512134]
42. Vaupel P, Horsman MR. Tumour perfusion and associated physiology: characterization and significance for hyperthermia. Int J Hyperthermia. 2010; 26(3):209–210. [PubMed: 20388020]
43. Jansen JFSH, Lee NY, Stambuk HE, Wang Y, Fury MG, Patel SG, Pfister DG, Shah JP, Koutcher JA, Shukla-Dave A. Tumor Metabolism and Perfusion in Head and Neck Squamous Cell Carcinoma: Pretreatment Multimodality Imaging with (1)H Magnetic Resonance Spectroscopy, Dynamic Contrast-Enhanced MRI, and [(18)F]FDG-PET. Int J Radiat Oncol Biol Phys. 2011
44. Lammers T, Kiessling F, Hennink WE, Storm G. Nanotheranostics and image-guided drug delivery: current concepts and future directions. Molecular Pharmaceutics. 2010; 7(6):1899–1912. [PubMed: 20822168]
45. Lammers T, Aime S, Hennink WE, Storm G, Kiessling F. Theranostics Nanomedicine. Acc Chem Res. 2011; 44(10):1029–1038. [PubMed: 21545096]

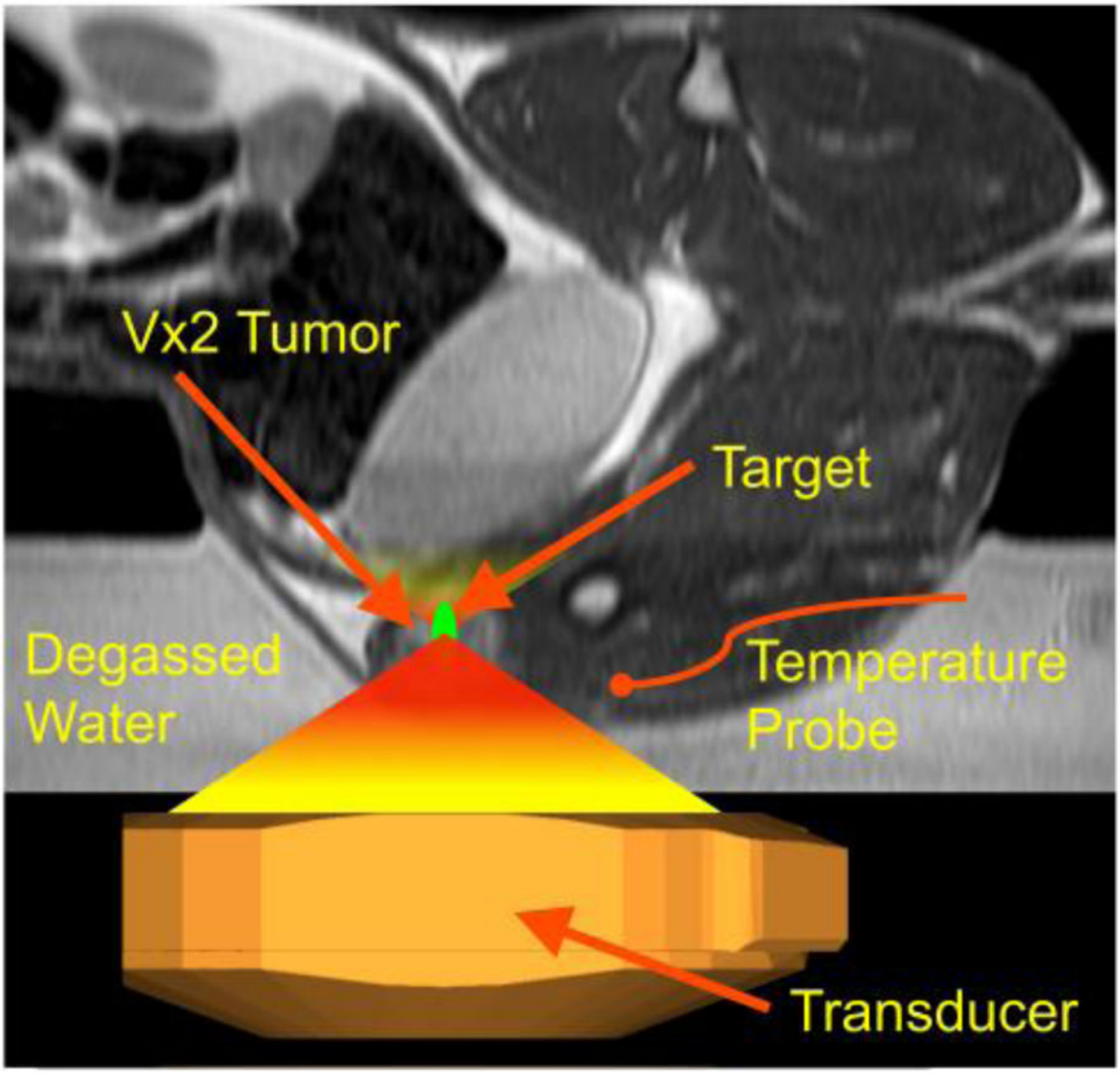

Fig.1.
Experimental setup for image-guided hyperthermia. Tumor-bearing right hind limb was submerged in degassed water and sonications were targeted (indicated by green ellipse) in the center of tumor. Reference temperature was obtained using an optical probe approximately displayed on the image.

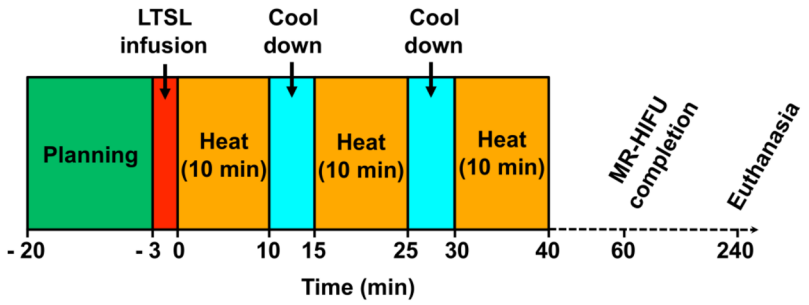

Fig.2.

Schematic representation of MR-HIFU experimental time line for image guided hyperthermia: Following acquisition of planning images and a slow infusion of LTSL, hyperthermia (10 min) was interleaved with 5-min cooling periods. This was repeated for a total of 3 treatments or until 30 min of heating was achieved within 1 hour after drug infusion. Rabbits were euthanized 4 hours after LTSL infusion and tissues were harvested for HPLC or histological analysis.

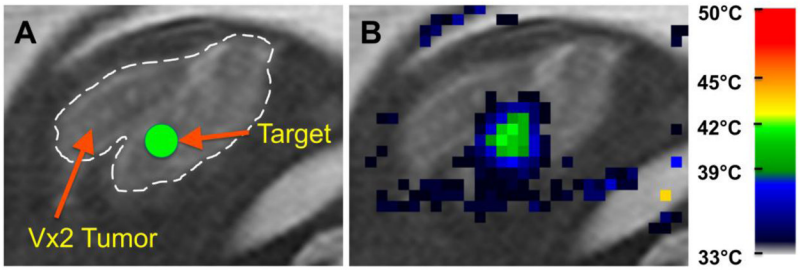

Fig.3. Planning and temperature mapping for image-guided hyperthermia

A) The Vx2 tumor was clearly identified on the planning images and a treatment target (diameter = 4 mm) was placed in the middle of the tumor (green circle), avoiding bone, vessels and fascial planes when possible. B) Real-time temperature monitoring using the proton resonance frequency shift method shown in color overlaid on the planning image (grayscale).

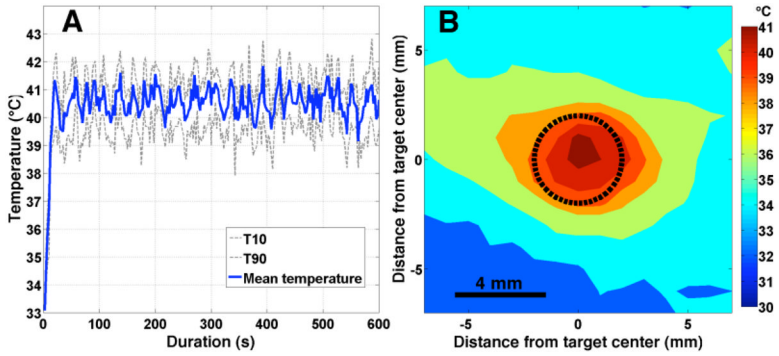

Fig.4. Image guided hyperthermia

Representative examples of temperature elevation and spatial distribution during a sonication. A) Following a short heat-up period (~20s), stable mild hyperthermia was achieved in the target region through binary feedback control. B) Time averaged spatial distribution of temperature in the target region (black circle) and the surrounding tissue, showing a uniformity of elevated temperature in the target region.

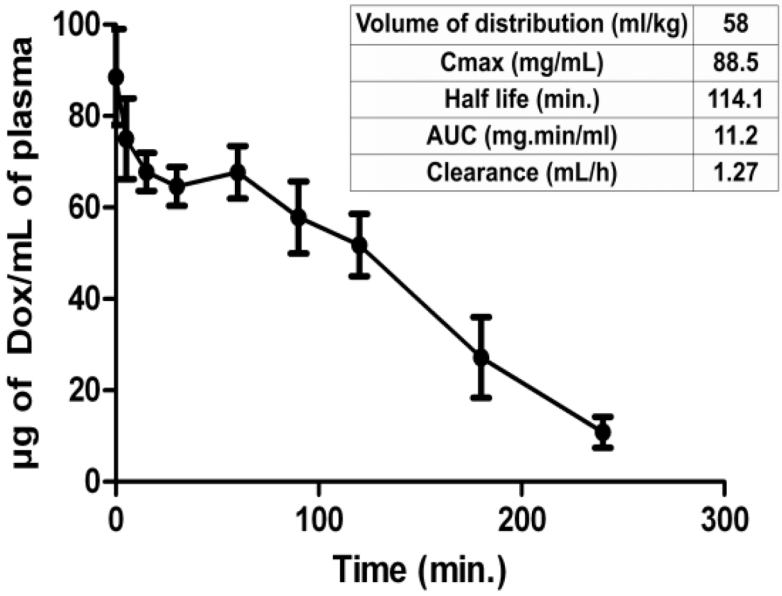

Fig. 5.

Pharmacokinetic profile in rabbits, following slow intravenous infusion of LTSL for 3 min. at a dose of 5 mg/kg doxorubicin. Data are shown as mean doxorubicin concentration in plasma with standard error of mean (n=3). Pharmacokinetic parameters were determined with a standard non-linear regression analysis assuming one compartment.

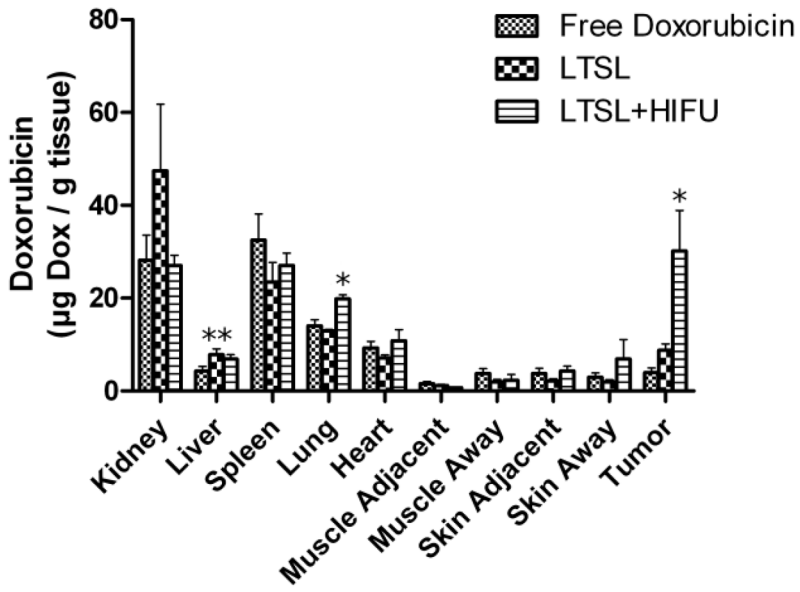

Fig. 6.

Biodistribution of doxorubicin in rabbits 4 h following treatment with doxorubicin alone, LTSL or LTSL+MR-HIFU at a dose of 5 mg/kg doxorubicin. Data are shown as mean doxorubicin concentration in the indicated tissues with standard error of mean (n=5). *Free Dox & LTSL vs LTSL + MR-HIFU; ** Free Dox vs LTSL, $p<0.05$

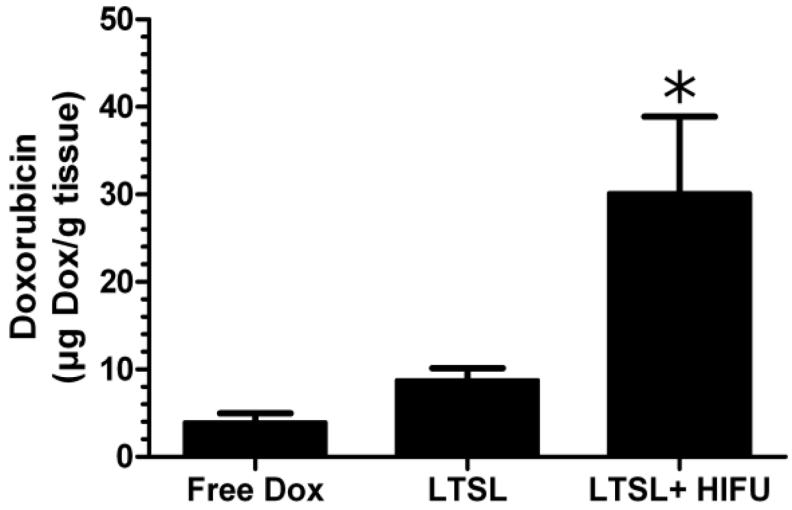

Fig. 7.

Doxorubicin detected in rabbit tumor following treatment either with free doxorubicin, LTSL or LTSL+MR-HIFU at a dose of 5 mg/kg doxorubicin. Data are shown as mean doxorubicin concentration in the tumor with standard error of mean (n=5). * $p<0.05$.

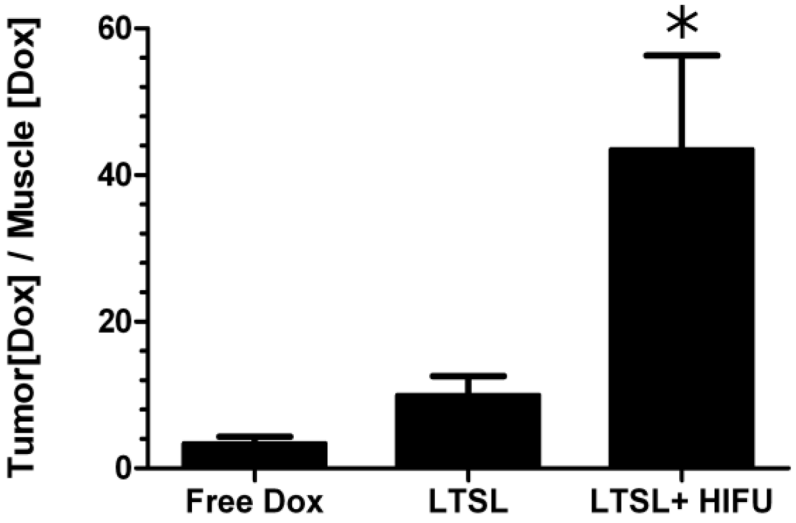

Fig. 8.

Specificity of drug delivery shown by relative doxorubicin concentration in rabbit tumor as compared to adjacent muscle following treatment either with free doxorubicin, LTSL or LTSL+MR-HIFU at a dose of 5 mg/kg doxorubicin. Data are shown as mean doxorubicin concentration in the tumor with standard error of mean (n=5). * $p<0.05$.

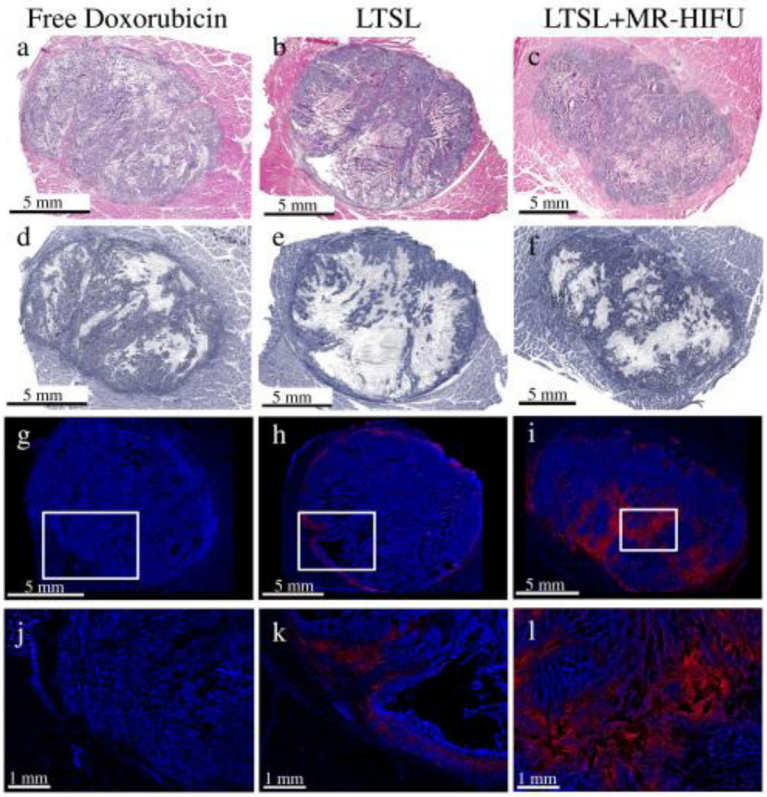

Fig. 9.

Histological and fluorescence analysis of Vx2 hindlimb tumors following treatment. A-c) H&E staining of tumor encased in muscle; d-f) NBT viability staining of tumors (viable = blue/purple, clear/white = cellular death); g–l) Fluorescence images of doxorubicin distribution with location of higher magnification shown by the box (nuclei:blue and Doxorubicin: red).

Table 1

Analysis of the tumor and organ doxorubicin at 4 h post treatment

Organ	Free Doxorubicin		LTSL		LTSL + MR-HIFU	
	Doxorubicin Quantified, μg/g (Mean (SEM)	% ID/g tissue (Mean [SEM])	Doxorubicin Quantified, μg/g (Mean (SEM)	% ID/g tissue (Mean [SEM])	Doxorubicin Quantified, μg/g (Mean (SEM)	% ID/g tissue (Mean [SEM])
Liver	4.3 (1.0)	0.028 (0.008)	7.8 (1.2)	0.051 (0.009)	6.9 (0.9)	0.044 (0.006)
Spleen	32 (6)	0.20 (0.03)	24 (4)	0.15 (0.03)	27 (3)	0.17 (0.02)
Lung	14.1 (1.3)	0.089 (0.008)	13.0 (0.3)	0.083 (0.005)	19.8 (0.9)	0.125 (0.007)
Heart	9.3 (1.4)	0.06 (0.009)	7.1 (0.7)	0.046 (0.006)	11 (2)	0.067 (0.015)
Muscle Adjacent	1.6 (0.5)	0.010 (0.003)	1.2 (0.3)	0.0071 (0.0014)	0.73 (0.06)	0.0050(0.0003)
Muscle Away	3.8 (1.1)	0.024 (0.007)	2.0 (0.6)	0.012 (0.003)	2.3 (1.3)	0.014 (0.008)
Skin Adjacent	3.7 (1.2)	0.026 (0.004)	2.1 (0.5)	0.014 (0.003)	4.3 (1.1)	0.027 (0.007)
Skin Away	3.0 (1.0)	0.018 (0.012)	2.0 (0.4)	0.013 (0.003)	7 (4)	0.04 (0.03)
Kidney	28 (5)	0.18 (0.08)	47 (14)	0.29 (0.08)	27 (2)	0.170 (0.014)
Tumor	3.9 (1.0)	0.023 (0.004)	8.8 (1.4)	0.061 (0.012)	30 (9)	0.26 (0.08)

J Control Release. Author manuscript; available in PMC 2013 March 28.